

Supplemental information

Antimicrobial overproduction sustains intestinal inflammation by inhibiting *Enterococcus* colonization

Kyung Ku Jang, Thomas Heaney, Mariya London, Yi Ding, Gregory Putzel, Frank Yeung, Defne Ercelen, Ying-Han Chen, Jordan Axelrad, Sakteesh Gurunathan, Chaoting Zhou, Magdalena Podkowik, Natalia Arguelles, Anusha Srivastava, Bo Shopsin, Victor J. Torres, A. Marijke Keestra-Gounder, Alejandro Pironti, Matthew E. Griffin, Howard C. Hang, and Ken Cadwell

Supplemental Figure 1

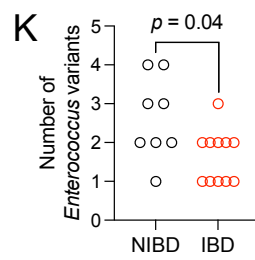
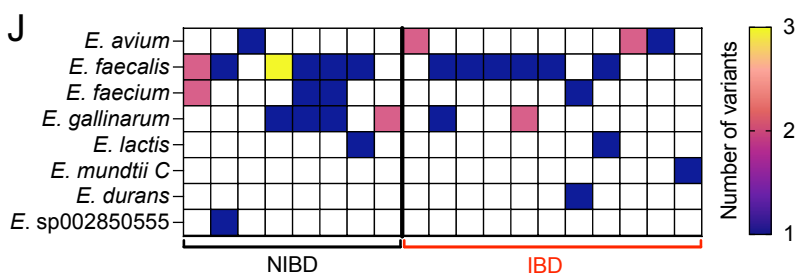
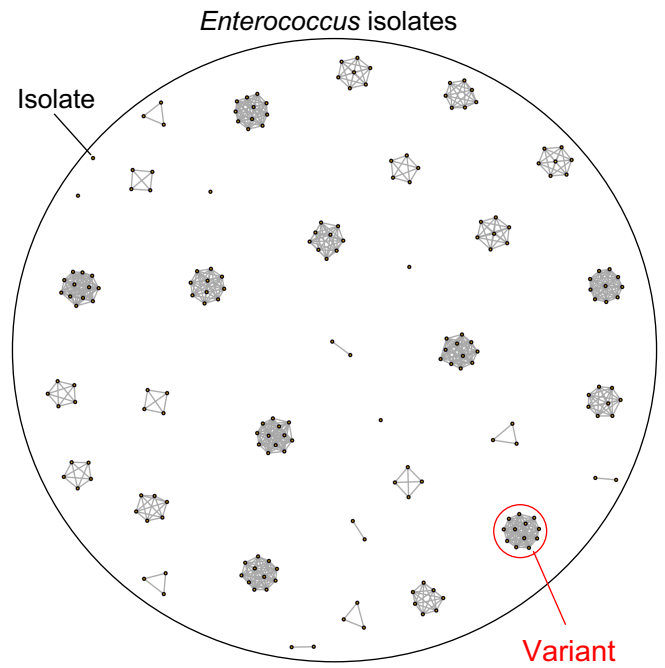
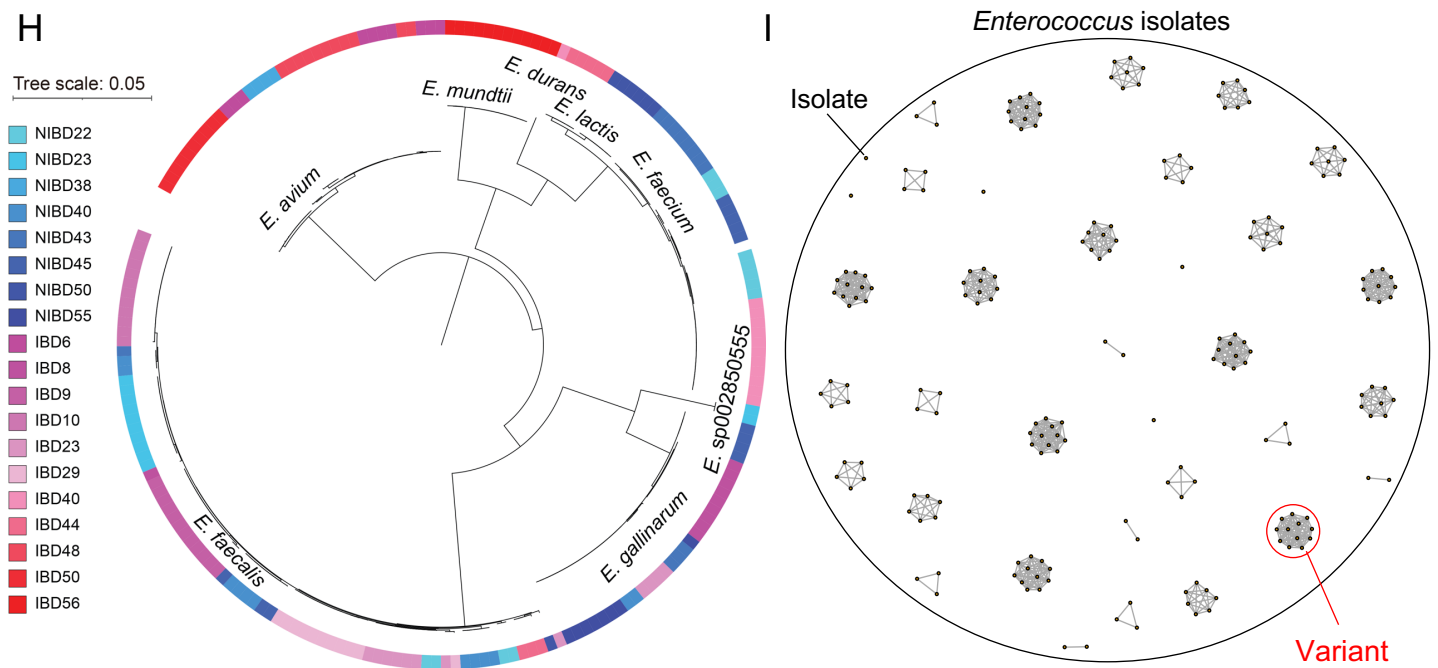
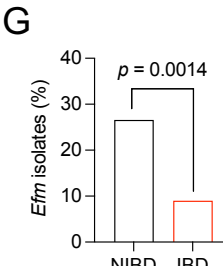
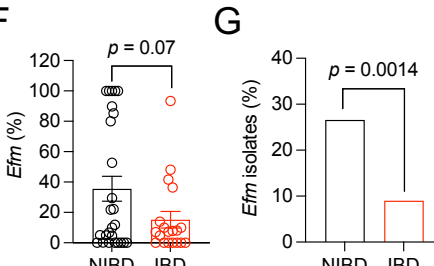
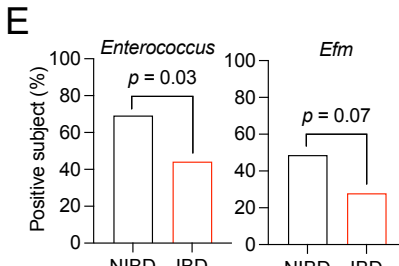
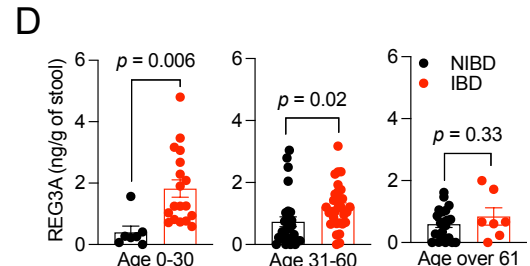
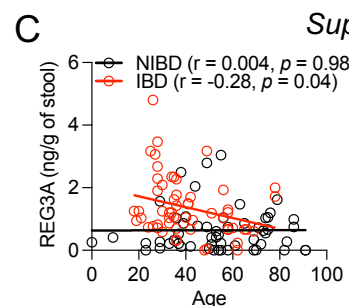
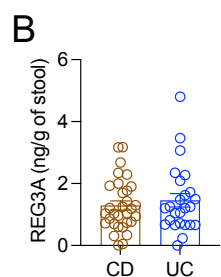
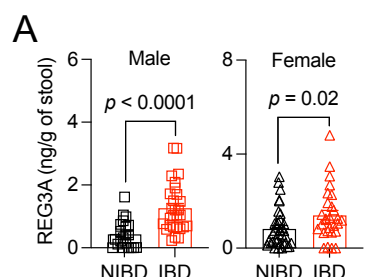


Figure S1. Contribution of patient demographics to REG3A levels and antimicrobial activity and genomic analysis of *Enterococcus* isolates from non-IBD (NIBD) and IBD patients, Related to Figures 1 and 2 and Tables S1-S3. **A)** REG3A concentration in stool extracts from NIBD and IBD patients from Figure 1 separated by sex. **B)** REG3A concentration in stool extracts from Crohn's disease (CD) or ulcerative colitis (UC) patients. **C)** Correlation between age of NIBD and IBD patients and REG3A concentration. **D)** REG3A concentration in stool extracts segregated into indicated age groups. **E)** Proportion of patients in which *Enterococcus* (left) and *E. faecium* (*Efm*, right) were detected in stool. **F)** Proportion of *Enterococcus* that are *Efm* in NIBD and IBD stools. **G)** Proportion of *Efm* isolates from the *Enterococcus* isolates (n = 79 for NIBD and n = 122 for IBD) of NIBD (n = 8) and IBD (n = 11) patients. **H)** Phylogenetic tree and source of *Enterococcus* isolates. **I)** Clustering of *Enterococcus* isolates that carried less than 100 single nucleotide polymorphisms (SNPs). Each dot and cluster indicate a single *Enterococcus* isolate and *Enterococcus* variant, respectively. Lines indicate pairs of isolates differing by no more than 100 SNPs. **J)** Heatmap displaying the individual-level diversity of *Enterococcus* variants in NIBD and IBD patients. Color indicates the number of variants found. **K)** Number of *Enterococcus* variants in NIBD and IBD patients. Data points in A-D, F, and K represent individual patients. Bars represent mean \pm SEM and at least two independent experiments were performed. r, Pearson correlation coefficient. Indicated p values by unpaired t test, two-tailed in A, D, and F, simple linear regression analysis in C, Fisher's exact test in E and G, and Wilcoxon rank sum test in K.

Supplemental Figure 2

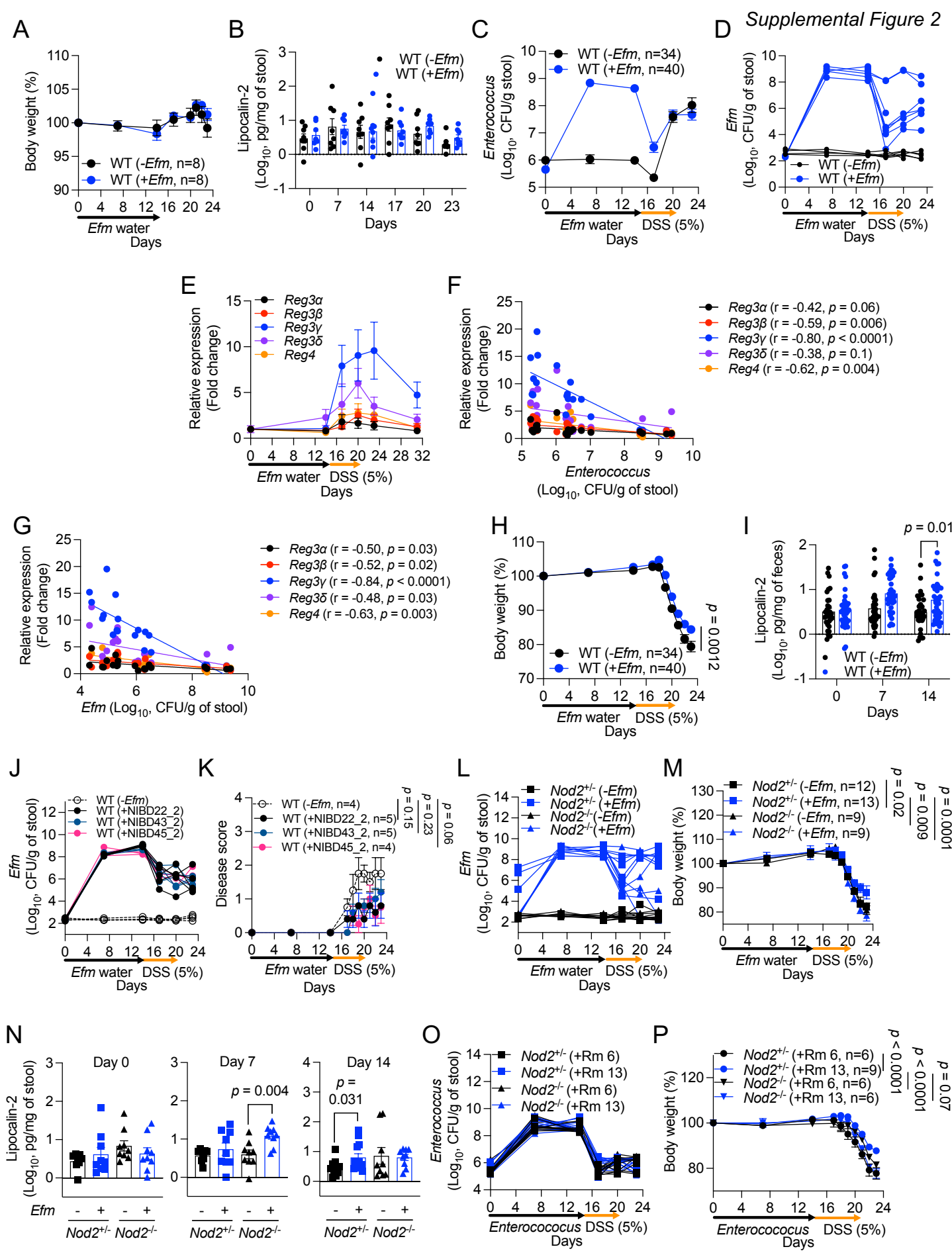


Figure S2. Colonization levels, *Reg* family gene expression, and disease parameters of mice inoculated with *Efm*, Related to Figure 3 and Table S4. **A and B)** Changes in body weight (A) and fecal lipocalin-2 (LCN2) (B) in wild-type (WT) B6 mice following administration of *Efm* or control. **C-I)** Dextran sulfate sodium (DSS)-induced intestinal injury of WT mice from room 6 (Rm 6) following administration of *Efm* (C-I) or control. The mice were examined for changes in burden of total *Enterococcus* (C) and *Efm* (D) in the stool, expression of *Reg3 α* , *Reg3 β* , *Reg3 γ* , *Reg3 δ* , and *Reg4* in colonic tissue (E), correlation between *Reg* gene expression and total *Enterococcus* (F) or *Efm* (G), changes in body weight (H), and fecal LCN2 (I). **J and K)** *Efm* burden (J) and disease score change (K) after DSS treatment of WT mice from Rm 6 following administration of *Efm* isolates from NIBD patients. **L-N)** DSS-treatment of *Nod2^{+/-}* and *Nod2^{-/-}* mice from Rm 6 following administration of *Efm* or control. The mice were examined for *Efm* burden in stool samples (L), changes in body weight (M), and fecal LCN2 (N) **O and P)** total *Enterococcus* burden (O) and body weight change (P) after DSS treatment of *Nod2^{+/-}* and *Nod2^{-/-}* mice following administration of *Enterococcus* isolated from Rm 6 or Rm 13. Data points in B, F, G, I, and N and lines in D, J, L, and O represent individual mice. Data points in C, E, H, K, M, and P represent mean \pm SEM. Bars represent mean \pm SEM and at least two independent experiments were performed. r, Pearson correlation coefficient. Indicated p values by simple linear regression analysis in F and G, two-way ANOVA test in H, K, M and P, and unpaired t test, two-tailed in I and N.

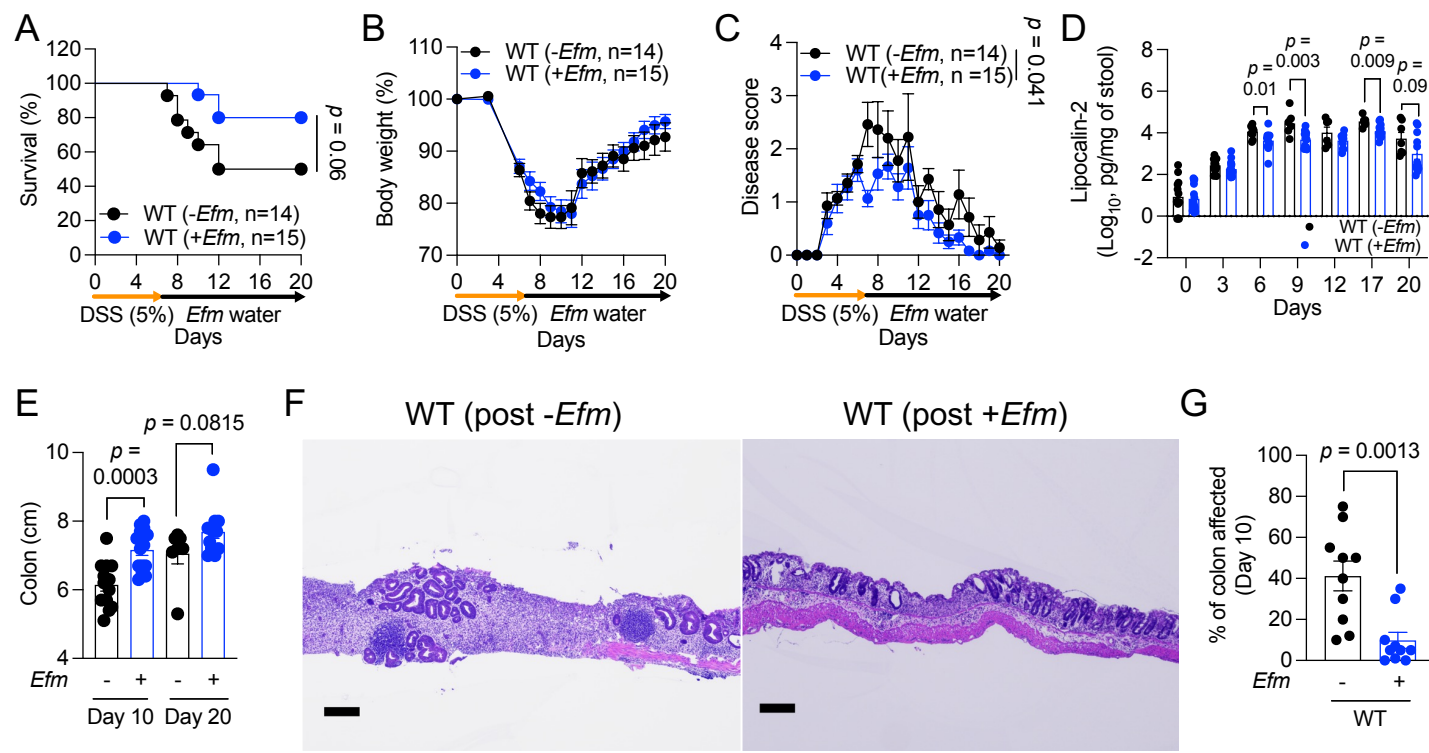


Figure S3. Amelioration of intestinal injury in mice by *Efm* inoculation after DSS administration, Related to Figure 3 and Table S4. A-E) WT B6 mice from Rm 6 received *Efm* or control following DSS treatment. The mice were examined for survival (A), changes in body weight (B) and disease score (C), fecal LCN2 (D), and colon length on days 10 and 20 (E). F and G) Representative images of hematoxylin and eosin (H&E)-stained sections of the colon (F) and quantification of the proportion of colon affected (G) on day 10 from mice in A-E. Bars, 200 μ M. Data points in D, E, and G represent individual mice. Data points in B and C represent mean \pm SEM. Bars represent mean \pm SEM and at least three independent experiments were performed. Indicated *p* values by log-rank Mantel-Cox test in A, two-way ANOVA test in C, and unpaired *t* test, two-tailed in D, E, and G.

Supplemental Figure 4

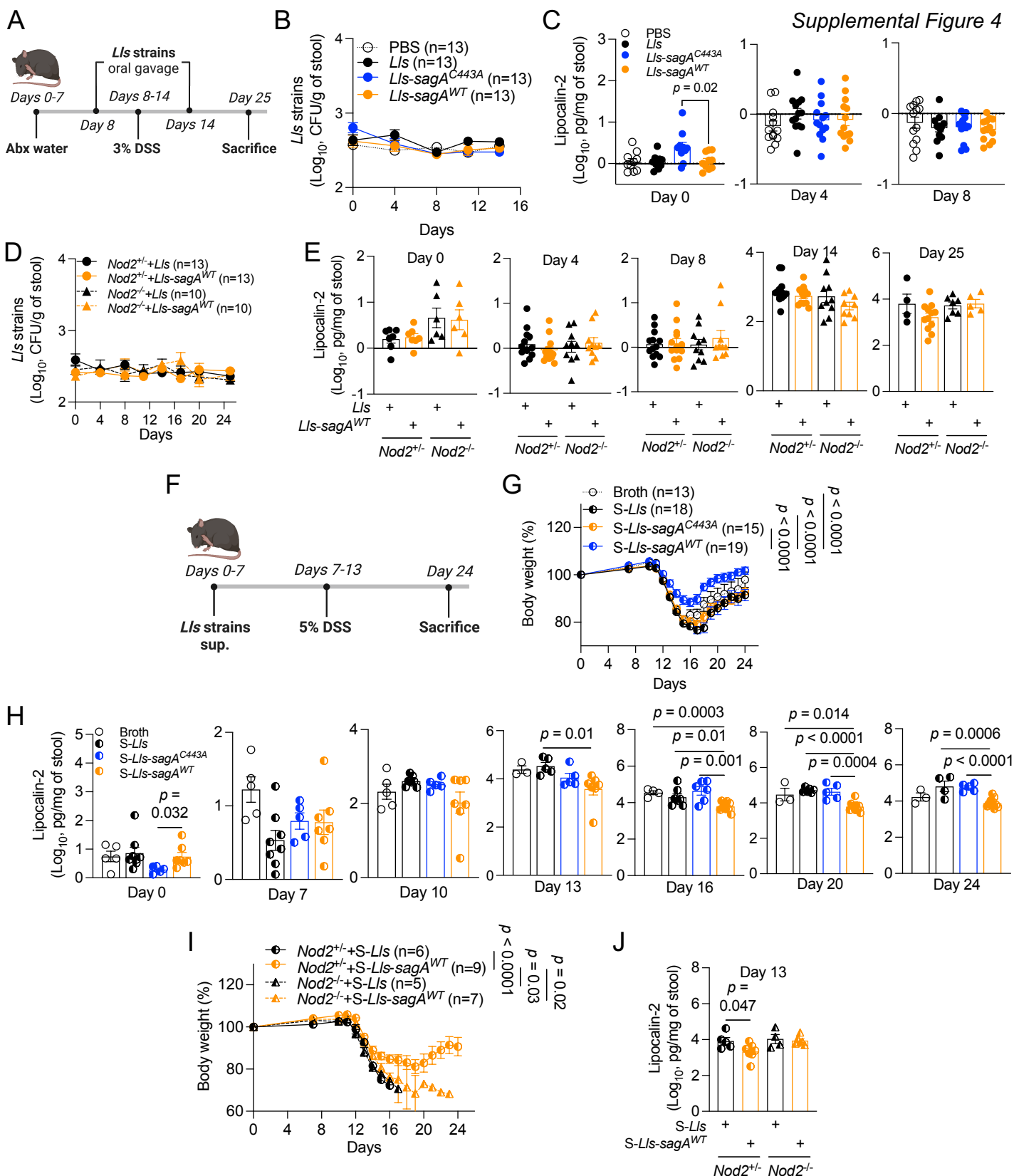


Figure S4. *Lactococcus lactis* expressing SagA promotes NOD2-dependent protection against intestinal injury, Related to Figure 4. **A)** Schematic of experimental procedure for mice inoculation with *L. lactis* (*L/l*s) strains. Mice received antibiotics (ampicillin + streptomycin, abx) for 7 days, and were orally gavaged with PBS or *L/l*s strains twice on days 8 and 14 to coincide with the initiation and cessation of DSS administration. **B and C)** Abx-treated WT mice given PBS, parental *L/l*s, *L/l*s expressing catalytic mutant SagA (*L/l*s-sagA^{C443A}), or *L/l*s expressing WT SagA (*L/l*s-sagA^{WT}) were treated with DSS as in A and examined for the burden of *L/l*s strains (B) and fecal LCN2 (C). **D and E)** Abx-treated *Nod2*^{+/-} and *Nod2*^{-/-} mice given parental *L/l*s or *L/l*s-sagA^{WT} were treated with DSS and examined for the burden of *L/l*s strains (D) and fecal LCN2 (E). **F)** Schematic of experimental procedure for DSS treatment of mice that received broth or culture supernatants of *L/l*s strains. **G and H)** DSS-treatment of WT mice inoculated with broth or culture supernatants of *L/l*s (S-*L/l*s), *L/l*s-sagA^{C443A} (S-*L/l*s-sagA^{C443A}), or *L/l*s-sagA^{WT} (S-*L/l*s-sagA^{WT}) were examined for changes in body weight (G) and fecal LCN2 (H). **I and J)** DSS-treatment of *Nod2*^{+/-} and *Nod2*^{-/-} mice inoculated with S-*L/l*s or S-*L/l*s-sagA^{WT}. The mice were examined for changes in body weight (I) and fecal LCN2 on day 13 (J). All mice were bred in Rm 6. Data points in C, E, H, and J represent individual mice. Data points in B, D, and I represent mean ± SEM. Bars represent mean ± SEM and at least two independent experiments were performed. Indicated *p* values by unpaired *t* test, two-tailed in C, H, and J and two-way ANOVA test in G and I.

Supplemental Figure 5

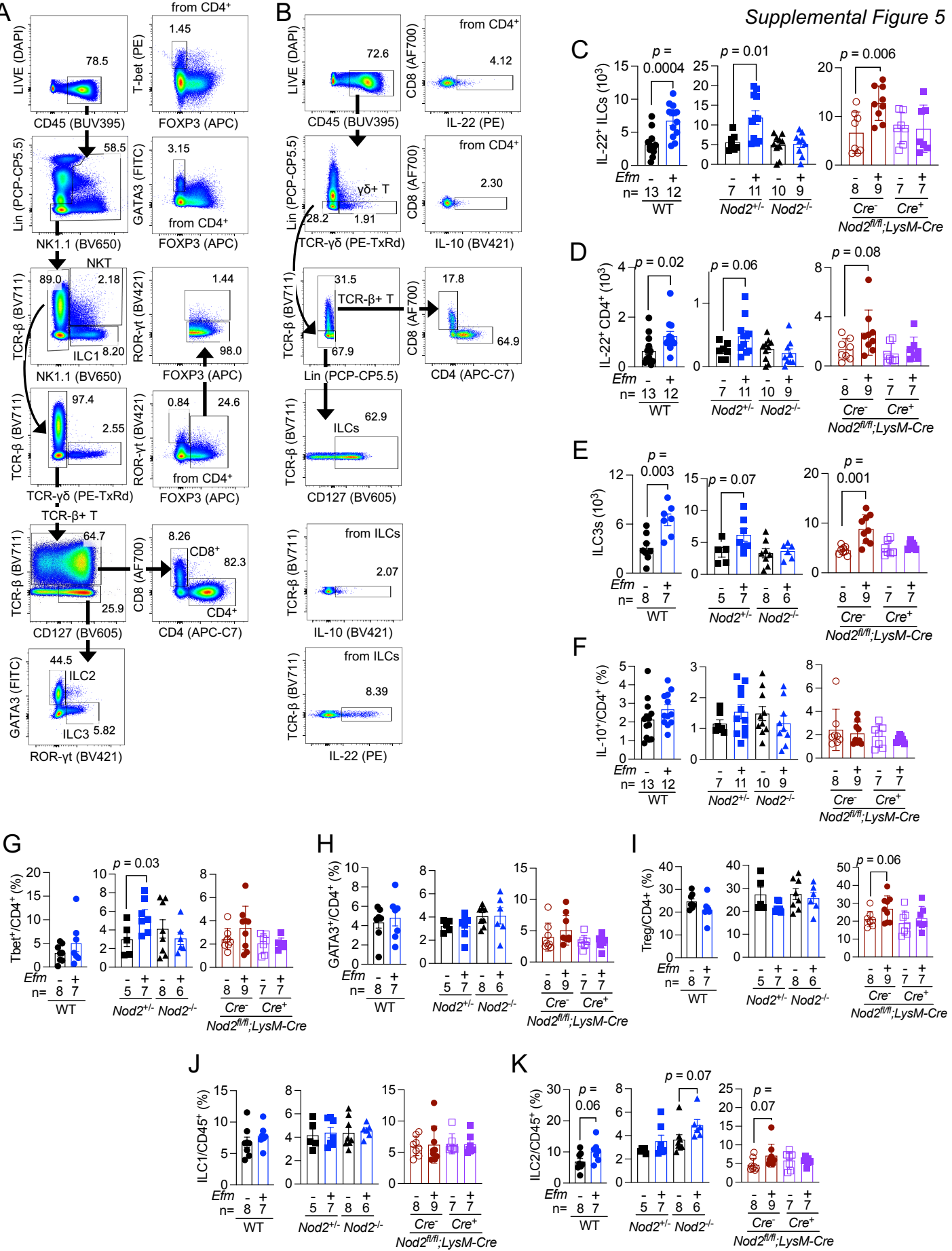


Figure S5. Immune cell analysis of colons from *Efm*-colonized mice, Related to Figure 6. A and B) Flow cytometry gating strategies for T cells and innate lymphoid cells (ILCs) (A, transcription factors), and cytokine production (B). **C-E**) Quantification of the number of IL-22⁺ ILCs (C) and CD4⁺ T helper cells (D) and group 3 ILCs (ILC3s, E) in WT, *Nod2*^{+/-}, *Nod2*^{-/-}, and *Nod2*^{f/f};LysM-Cre⁻ and Cre⁺ mice following administration of *Efm* or control. **F-K**) Flow cytometric quantification of the proportion of IL10⁺ (F), Tbet⁺ (G), and GATA3⁺ (H) CD4⁺ T cells, regulatory T cells (Treg, I), ILC1 (J), and ILC2 (K) in WT, *Nod2*^{+/-}, *Nod2*^{-/-}, and *Nod2*^{f/f};LysM-Cre⁻ and Cre⁺ mice following 2-week administration of *Efm* or control. Data points in C-K represent individual mice. Bars represent mean ± SEM and at least two independent experiments were performed. Indicated *p* values by unpaired *t* test, two-tailed in C-E, G, I, and K.

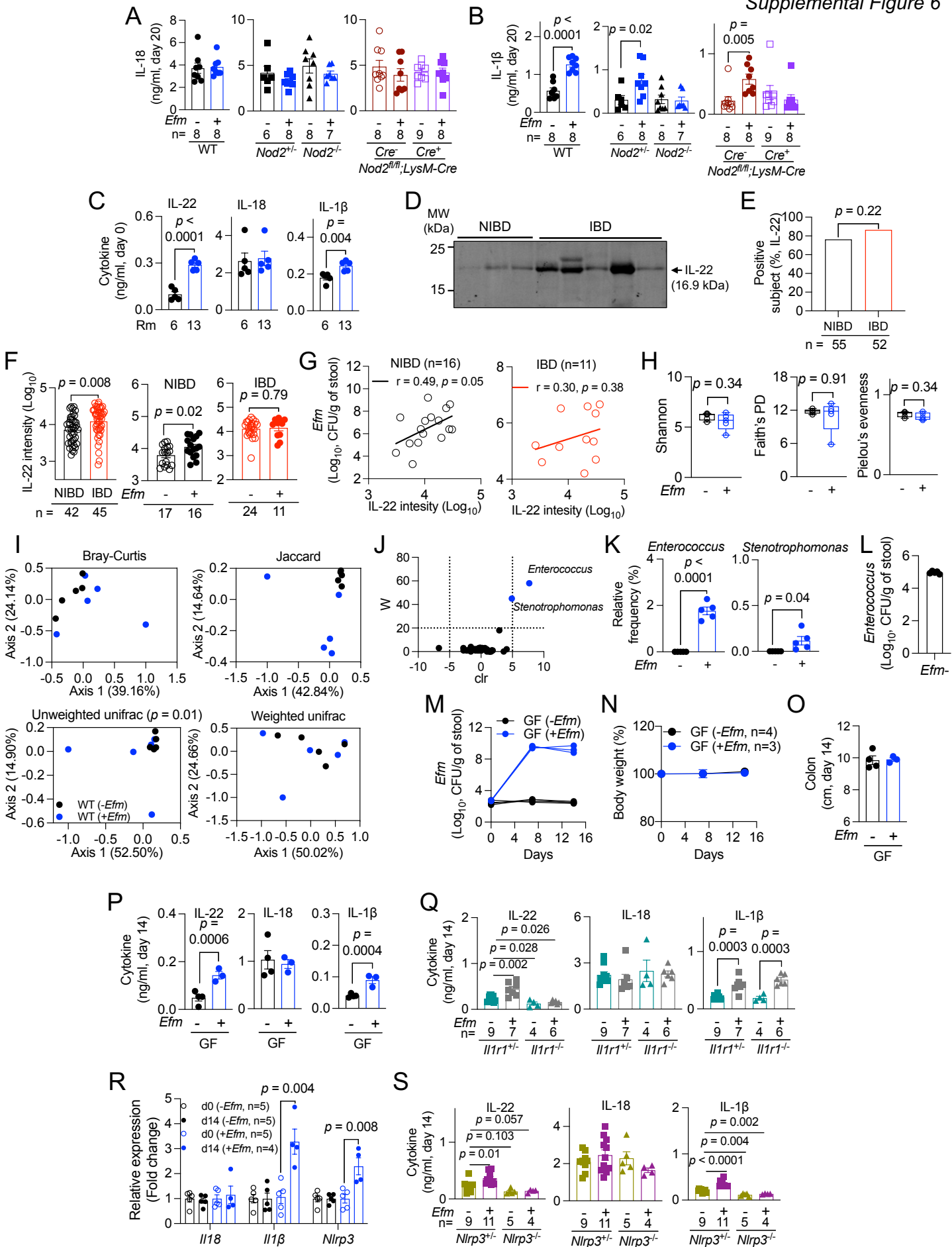


Figure S6. Analyses of cytokines and microbiota composition of *Efm*-colonized mice and IL-22 in human stool extracts, Related to Figure 6 and Tables S1 and S2. A and B)

Quantification of secreted IL-18 (A) and IL-1 β (B) in gut explants from *Efm*-colonized WT, *Nod2*^{+/-}, *Nod2*^{-/-}, and *Nod2*^{fl/fl};LysM-Cre⁻ and Cre⁺ mice on day 20. **C)** Quantification of IL-22 (left), IL-18 (middle), and IL-1 β (right) in gut explants from Rm 6 ($n = 5$) or Rm 13 mice ($n = 5$). **D)** Western blot of IL-22 in stool extracts from representative 3 NIBD and 5 IBD patients. **E)** Proportion of stool specimens from NIBD and IBD patients in which IL-22 was detectable by Western blot. **F)** Band intensity of IL-22 from NIBD and IBD patients (left) and segregation of NIBD (middle) or IBD (right) patients according to *Efm* positivity. **G)** Correlation between IL-22 band intensity and *Efm* burden from NIBD (left) or IBD (right) patients. **H-K)** 16S rRNA sequencing of stool from WT mice following administration of *Efm* or control. Alpha diversity values calculated as Shannon (left), Faith's phylogenetic diversity (PD) (middle), and Pielou's evenness (right) indices (H). Principle coordinate analyses of beta diversity determined by Bray-Curtis, Jaccard, and Unweighted and Weighted unifrac methods (I). Differentially abundant microbial taxa identified by analysis of composition of microbiomes (ANCOM) (J). Clr (x-axis) is a measure of the effect size difference for a particular species between the two conditions. W (y-axis) is the strength of the ANCOM for the tested number of species. Proportion of sequencing reads representing *Enterococcus* (left) and *Stenotrophomonas* (right) in *Efm*-colonized mice (K). **L)** Burden of endogenous *Enterococcus* in mice receiving control water in H-K. **M-P)** *Efm* burden in stool (M), changes in body weight (N), colon length on day 14 (O), and IL-22 (left), IL-18 (middle), and IL-1 β (right) in gut explants on day 14 (P) in germ-free (GF) WT mice following oral administration with *Efm* or control on day 0. **Q)** Quantification of IL-22 (left), IL-18 (middle), and IL-1 β (right) in the supernatants of gut explants from *Efm*-colonized *Il1r1*^{+/-} or *Il1r1*^{-/-} mice on day 14. **R)** qRT-PCR analysis of *Il18*, *Il1 β* , and *Nlrp3* expression in colonic tissue from Rm 6 WT mice following 2-week administration of *Efm* or control. **S)** Quantification of IL-22 (left), IL-18 (middle), and IL-1 β (right) in gut explants from *Efm*-colonized *Nlrp3*^{+/-} or *Nlrp3*^{-/-} mice on day 14. Data points in A-C, H, I, K, L, and O-S and lines in M represent individual mice. Data points in F and G represent individual patients. Data points in N represent mean \pm SEM. Bars represent mean \pm SEM and at least two independent experiments were performed. r, Pearson correlation coefficient. Indicated p values by unpaired t test, two-tailed in B, C, F, K, and P-S, Fisher's exact test in E, simple linear regression analysis in G, Kruskal-Wallis test in H, and permutational multivariate analysis of variance in I.

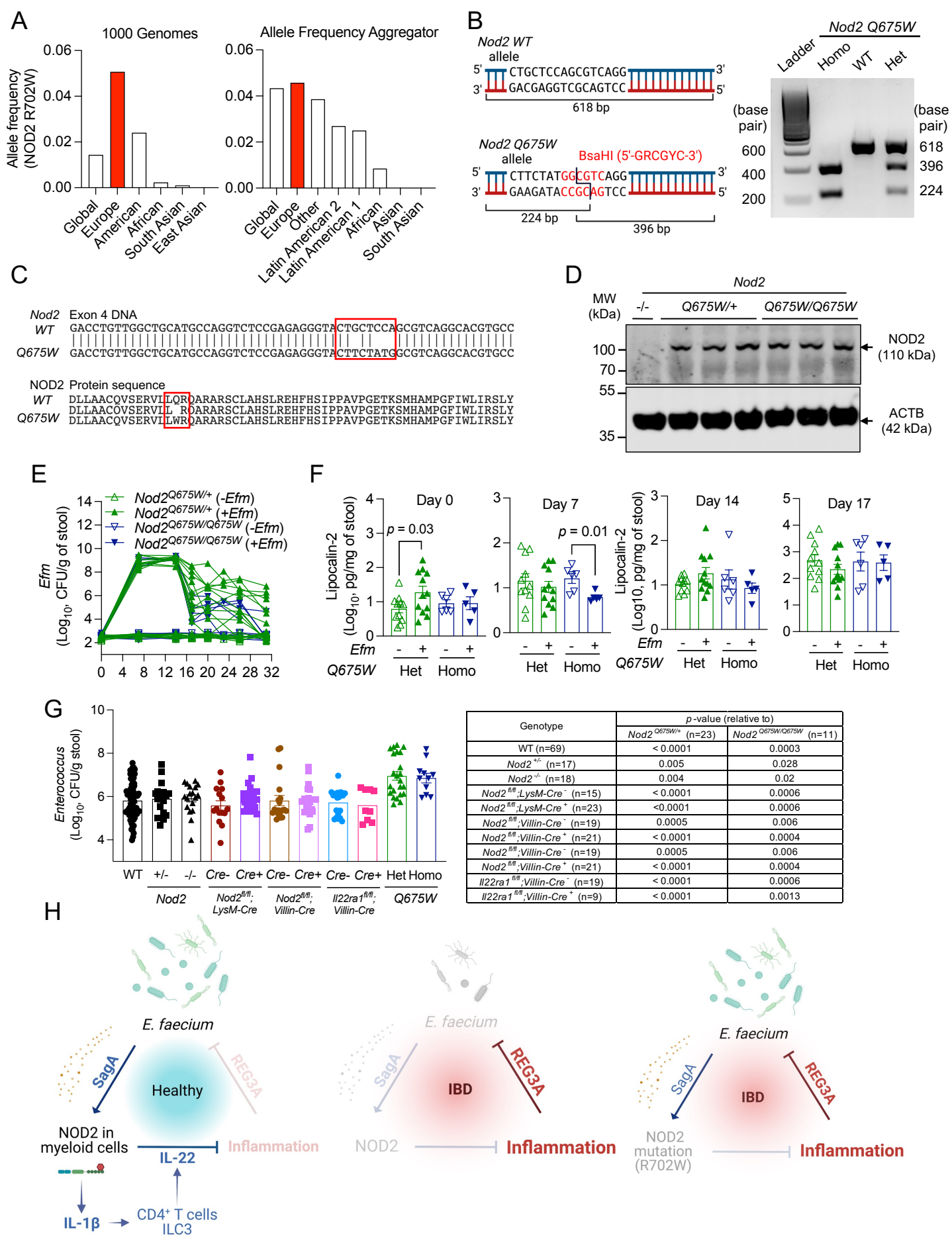


Figure S7. Characterization of mice carrying a *Nod2* knock-in mutation equivalent to the human R702W, Related to Figure 7 and Table S4. **A)** *NOD2 R702W* allele frequency according to ethnic groups. The frequencies were retrieved from 1000 Genomes Project and Allele Frequency Aggregator. **B)** Schematic of genotyping PCR product (left) and representative genotyping gel image (right) for *Nod2 Q675W* knock-in mouse. **C)** Sequencing of the *Nod2* locus from the above mice confirmed successful gene targeting. Figure shows exon 4 DNA and amino acid sequences from *Nod2 Q675W* knock-in mouse sequencing results aligned to the WT sequences. Red boxes indicate the mutated region. **D)** Western blot image of *NOD2* and β -actin (ACTB) in colonic tissue lysates from *Nod2*^{-/-}, *Nod2*^{Q675W/+}, and *Nod2*^{Q675W/Q675W} mice. **E and F)** DSS treatment of *Nod2*^{Q675W/+} and *Nod2*^{Q675W/Q675W} mice from Rm 6 following 2-week administration of *Efm* or control. The mice were examined for the burden of *Efm* (E) and fecal LCN2 (F). **G)** Endogenous *Enterococcus* burden among mice with different genotypes on day 0 (upper). The *p*-values relative to *Nod2*^{Q675W/+} or *Nod2*^{Q675W/Q675W} mice were indicated in lower table. **H)** Schematic of the mechanism by which *Efm* activates *NOD2* to suppress inflammation, and how this process is disrupted when either *REG3A* is overproduced or *NOD2* is genetically inactivated. Lines in E and data points in F and G represent individual mice. Bars in F and G represent mean \pm SEM and at least three independent experiments were performed. Het, heterozygotes; Homo, homozygotes. Indicated *p* values by unpaired *t* test, two-tailed in F and G.